Textural Characterization of Micro- and Mesoporous Carbons Using Combined Gas Adsorption and n-Nonane Preadsorption

ARTICLE *in* LANGMUIR · MAY 2013

Impact Factor: 4.46 · DOI: 10.1021/la401206u · Source: PubMed

6 AUTHORS, INCLUDING:

Lars Borchardt
Technische Universität Dresden
62 PUBLICATIONS **1,522** CITATIONS
SEE PROFILE

Francisco Rodriguez-Reinoso
University of Alicante
397 PUBLICATIONS **9,877** CITATIONS
SEE PROFILE

Stefan Kaskel
Technische Universität Dresden
295 PUBLICATIONS **6,825** CITATIONS
SEE PROFILE

J. Silvestre-Albero
University of Alicante
106 PUBLICATIONS **2,051** CITATIONS
SEE PROFILE

Langmuir

Article

pubs.acs.org/Langmuir

Textural Characterization of Micro- and Mesoporous Carbons Using Combined Gas Adsorption and *n*-Nonane Preadsorption

Martin Oschatz,[†] Lars Borchardt,[†] Soledad Rico-Francés,[‡] Francisco Rodríguez-Reinoso,[‡] Stefan Kaskel,*[,†] and Joaquín Silvestre-Albero*[,‡]

[†]Department of Inorganic Chemistry, Dresden University of Technology, Bergstrasse 66, D-01062 Dresden, Germany

[‡]Laboratorio de Materiales Avanzados, Departamento de Química Inorgánica-Instituto Universitario de Materiales, Universidad de Alicante, Ap. 99, E-03080 Alicante, Spain

Supporting Information

ABSTRACT: Porous carbon and carbide materials with different structures were characterized using adsorption of nitrogen at 77.4 K before and after preadsorption of *n*-nonane. The selective blocking of the microporosity with *n*-nonane shows that ordered mesoporous silicon carbide material (OM-SiC) is almost exclusively mesoporous whereas the ordered mesoporous carbon CMK-3 contains a significant amount of micropores (~25%). The insertion of micropores into OM-SiC using selective extraction of silicon by hot chlorine gas leads to the formation of ordered mesoporous carbide-derived carbon (OM-CDC) with a hierarchical pore structure and significantly higher micropore volume as compared to CMK-3, whereas a CDC material from a nonporous precursor is exclusively microporous. Volumes of narrow micropores, calculated by adsorption of carbon dioxide at 273 K, are in linear correlation with the volumes blocked by *n*-nonane. Argon adsorption measurements at 87.3 K allow for precise and reliable calculation of the pore size distribution of the materials using density functional theory (DFT) methods.

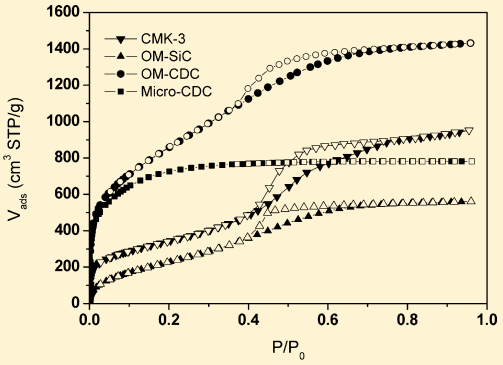

INTRODUCTION

Porous carbons[1,2] are used in many applications such as gas storage,[3,4] gas separation,[5] catalysis,[6,7] electrochemical energy storage,[8] or capacitive desalination.[9] Their qualification arises from chemical inertness, temperature stability, and, in parts, electric conductivity, all in combination with high specific surface areas mainly contributed by a huge amount of micropores (<2 nm).

The controlled integration of microporosity into carbon materials is therefore a permanent issue in present-day materials science. For instance, beside the physical and chemical activation of carbonaceous materials,[10] the selective extraction of metal atoms out of metal carbide matrixes has arisen to a powerful strategy for the directed synthesis of microporous carbons with a subangström accuracy.[11−13] Those materials are known as carbide-derived carbons (CDCs) and offer outstanding specific surface areas as high as 3000 m^2/g.

However, certain applications such as protein adsorption, drug delivery, or any application where larger molecules need to be adsorbed require larger pores, denoted as mesopores (2−50 nm).[14−17] These mesopores additionally favor enhanced materials transport within the porous structure and are therefore of significant importance. One well-known example for mesoporous carbon materials is called CMK (Carbon Mesostructured by Kaist).[18,19] This type of carbon exhibits an ordered arrangement of uniform sized pores, and it is synthesized by a hard-templating approach (also referred to as Nanocasting)[20,21] of sucrose into ordered mesoporous silica templates (OMS).

Both strategies, the CDC approach and the Nanocasting technique, have very recently been combined for the purpose of synthesizing a carbon material offering both, well-defined micro- and mesopores. These carbons are known as ordered mesoporous carbide-derived carbon (OM-CDC).[22] They are synthesized via the infiltration of polycarbosilane precursors into the pore system of OMS allowing for the formation of ordered mesoporous silicon carbide (OM-SiC). The silicon atoms can be selectively extracted using hot chlorine gas, thus leading to the formation of a large amount of micropores within the walls of the former mesoporous SiC. Since this transformation is highly conformal, the ordered mesopore structure is conserved. These carbons offer outstanding apparent surface areas as high as 3000 m^2/g, coupled with total pore volumes as high as 2.0 cm^3/g, and therefore, OM-CDCs are highly suitable in applications like gas storage, catalysis, capacitive deionization of water, and electrochemical energy storage.[22] In such adsorption related applications, the microporous carbon rods serve for high capacities, while the ordered mesopore system in between facilitates the access of the guest molecules to the adsorption sites. In consequence, OM-CDCs offer improved

Received: April 2, 2013
Revised: April 21, 2013
Published: May 23, 2013

kinetics in adsorption processes and advanced mass transfer behavior in electric double layer capacitor (EDLC) electrodes when compared to predominantly microporous CDCs or activated carbons.[22]

A clear understanding of the pore structure within such materials is of fundamental interest with regard to optimize them for the specific application. For instance, the ratio of micro- and mesopores in the hierarchical OM-CDC significantly influences the performance in gas adsorption and electrochemical energy storage. While advanced density functional theory (DFT) methods allow for a quite precise calculation of pore size distributions (PSDs) based on the adsorption of nitrogen (77.4 K) or argon (87.3 or 77.4 K), different DFT kernels drastically differ when the amount of micro- and mesopores is determined from the same isotherm. Previous studies showed that the nitrogen physisorption at 77.4 K before and after preadsorption of *n*-nonane, which selectively blocks the micropores, is a useful method to clearly distinguish between the contributions of micro- and mesopores to the porosity of materials such as ordered mesoporous silicas (OMS)[23] and hierarchical activated carbons.[24]

In this study we give a profound insight into the textural properties of different pores in micro- (CDC), meso- (CMK-3), and micro/mesoporous (OM-CDC) carbon materials.

We applied nitrogen physisorption, coupled with *n*-nonane preadsorption, for the determination of micro- and mesopore contributions in OM-SiC, OM-CDC, CMK-3, and a microporous CDC material. Carbon dioxide adsorption (273 K) confirms the selective blocking of micropores by the organic molecules. Additionally, argon adsorption (87.3 K) gives deep insights in the narrow micropore structure of the materials.

EXPERIMENTAL SECTION

Synthesis of SBA-15. First, 66.8 g of triblock copolymer Pluronic P123 ($EO_{20}PO_{70}EO_{20}$; $M_w \approx 5800$) was dissolved in 1212 g of distilled water at 308 K for 12 h followed by the addition of 38.6 g of 37% hydrochloric acid aqueous solution. After stirring for 1 h, 143.6 g of tetraethyl orthosilicate (TEOS) were subsequently added to the solution. After 24 h of stirring, the white dispersion underwent a hydrothermal treatment at 403 K for another 24 h. The resulting white powder was filtered, washed with a water/ethanol mixture (1:1 by volume), and finally calcined under air atmosphere at 823 K for 5 h.

Synthesis of Ordered Mesoporous Carbon (CMK-3). In a Petri dish, 2 g of the SBA-15 template were mixed with a 10 mL aqueous solution of 2.5 g of sucrose to which was added 0.28 g ofo 96% sulfuric acid. Polymerization of the hydrocarbon was achieved by heating the mixture to 373 K for 6 h followed by subsequent heating to 433 K for another 6 h. Complete infiltration of template pores was achieved by repeating the procedure described above with a 10 mL aqueous solution of 1.6 g of sucrose to which was added 0.18 g of 96% sulfuric acid, again followed by heating to 373 and 433 K. Carbonization was carried out under flowing argon atmosphere in a horizontal tubular furnace. The material was heated to 1173 K with a rate of 150 K/h and annealed for 2 h. Silica dissolution was achieved by treating the composite material in a hydrofluoric acid (35% aqueous solution)/water/ethanol mixture (1:1:1 by volume) for 3 h, followed by washing with large amounts of ethanol.

Synthesis of Ordered Mesoporous Silicon Carbide (OM-SiC). In a mortar, 2 g of the SBA-15 template were infiltrated with a mixture of 2.1 mL of liquid allylhydridopolycarbosilane SMP-10 and 0.5 mL of the cross-linker *para*-divinylbenzene by the incipient wetness method. Pyrolysis of the resulting SMP-10/SBA-15 composite was performed at 1073 K for 2 h with a heating rate of 60 K/h. Silica dissolution was achieved in the same way as compared to the above-described CMK-3 yielding a light brown powder.

Synthesis of Ordered Mesoporous Silicon Carbide-Derived Carbon (OM-CDC). OM-CDC was prepared by high temperature chlorine treatment of the OM-SiC precursor. Therefore, approximately 1 g of the mesoporous carbide was transferred into a quartz boat and placed in a horizontal tubular furnace equipped with a quartz tube. After flushing with 150 mL/min argon, the material was heated to 1073 K with a rate of 450 K/h. When reaching that value, the gas flow was changed to a mixture of 80 mL/min chlorine and 70 mL/min argon. After 3 h of chlorination, the furnace was cooled down to 873 K under an argon flow of 150 mL/min. At that temperature, the gas flow was changed to 80 mL/min hydrogen for 1 h with regard to remove chlorine and silicon chloride species adsorbed in the OM-CDC pores followed by cooling to room temperature under flowing argon.

Synthesis of Microporous CDC. SMP-10 was pyrolized at 973 K in a similar procedure as described for the OM-SiC. Chlorination was performed in analogy to the OM-CDC, but at a maximum temperature of 973 K. The postsynthetic hydrogen treatment was also carried out as described for the hierarchical material.

Characterization. N_2 adsorption isotherms before and after *n*-nonane preadsorption were performed in a homemade manometric equipment developed at the Advanced Materials Group (LMA), now commercialized as N_2Gsorb-6 (Gas to Materials Technologies; www.g2mtech.com). Preadsorption of *n*-nonane was performed in the manometric equipment described above using the following procedure: after degassing the material at 523 K for 4 h, the sample was exposed to *n*-nonane (Aldrich, 99%) for 30 min at 77.4 K and then left in contact with the liquid for 3 h at room temperature. After the preadsorption, the samples were degassed at 298 K overnight prior to the second measurement of the nitrogen isotherm.

The carbon dioxide measurements at 273 K as well as the argon adsorption measurements at 87.3 K were performed on a Quantachrome Autosorb 1C apparatus.

RESULTS AND DISCUSSION

The N_2 physisorption isotherms of ordered mesoporous silicon carbide (OM-SiC, which is the precursor material of the later hierarchical CDC) (Figure 1) as well as ordered mesoporous

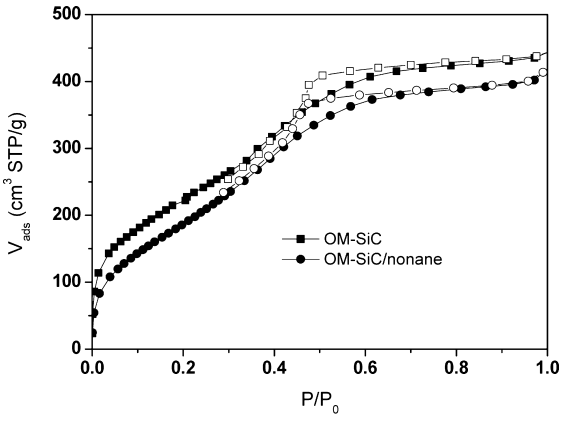

Figure 1. N_2 adsorption−desorption (filled symbols−empty symbols) isotherms at 77.4 K for ordered mesoporous silicon carbide (OM-SiC) before and after *n*-nonane preadsorption.

carbon (CMK-3) (Figure 2) show capillary condensation processes at medium relative pressures that are associated with the filling of the narrow mesopores present in both samples. The shape of the hysteresis loops is typical for mesoporous materials with an ordered arrangement of nanorods. While the adsorption branch reaches saturation at a relative pressure of $P/P_0 \approx 0.6$ for the OM-SiC, distinct nitrogen uptake takes place up to $P/P_0 \approx 0.7$ in CMK-3 indicating a slightly larger pore size within the carbon material. The N_2 physisorption isotherm of

dx.doi.org/10.1021/la401206u | *Langmuir* 2013, 29, 8133−8139

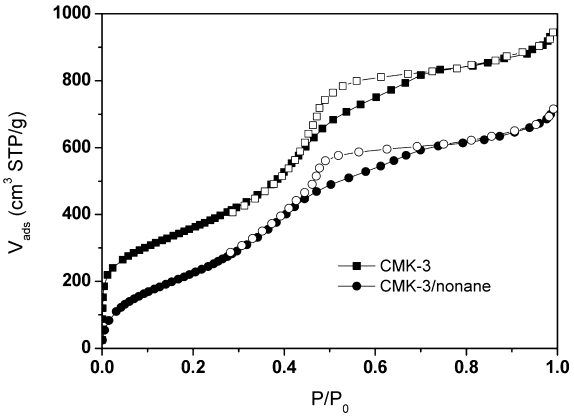

Figure 2. N_2 adsorption−desorption (filled symbols−empty symbols) isotherms at 77.4 K for ordered mesoporous carbon (CMK-3) before and after *n*-nonane preadsorption.

OM-SiC after *n*-nonane preadsorption (Figure 1) is nearly equal to the sample before hydrocarbon loading. *N*-Nonane blocks only 7% of the total pore volume indicating that this sample is almost exclusively mesoporous (Table 1). Besides a

Table 1. Porosity Property Summary of OM-SiC, CMK-3, OM-CDC, and Microporous CDC

sample	S_{BET} (m^2/g)	V_0 (cm^3/g)	V_{meso} (cm^3/g)	V_{Total} (cm^3/g)	V_n (cm^3/g)
OM-SiC	847	0.31	0.36	0.67	0.1
OM-SiC/*n*-nonane	723	0.24	0.39	0.62	–
CMK-3	1323	0.60	0.84	1.44	0.23
CMK-3/*n*-nonane	859	0.30	0.78	1.08	–
OM-CDC	2686	1.01	0.82	1.83	0.53
OM-CDC/*n*-nonane	1176	0.36	0.50	0.86	–
CDC-micro	2060	0.80	0.17	0.97	0.64
CDC-micro/*n*-nonane	110	0.03	0.04	0.07	–

slightly lower density of carbon compared to silicon carbide, the higher (mass-)specific surface area and pore volume of CMK-3 is associated with the presence of a certain amount of micropores and surface defects within the carbon nanorods. Therefore, the effect of *n*-nonane preadsorption on the nitrogen adsorption isotherm of the ordered mesoporous carbon is expected to be more important as compared to OM-SiC (see Figure 2). In this sense, the hydrocarbon molecules selectively block 25% of the total pore volume of CMK-3 belonging to micropores that are reasonable for the high specific surface area of this material (Table 1). Nevertheless, it can be summarized, that this sample can be regarded as being predominantly mesoporous.

In both materials, the mesopore structure is not affected by *n*-nonane blocking since the sizes, shapes, and positions of the hysteresis loops remain unchanged. This observation confirms that (i) *n*-nonane is effectively removed from the mesopores after the degassing treatment due to its lower adsorption potential, i.e., only micropores are blocked, and (ii) *n*-nonane blocking of the micropores has no effect on the N_2 capillary condensation/evaporation on the mesopores.

The selective extraction of the silicon atoms from OM-SiC leads to the formation of microporous carbide-derived carbon nanorods with a well-defined mesopore system between them (Scheme 1). The presence of this ordered mesopore structure was determined in recent studies by small-angle X-ray

Scheme 1. Schematic Illustration of the Synthesis Procedure and the Pore Structure of CMK-3, OM-SiC, and OM-CDC Materials Used in This Study

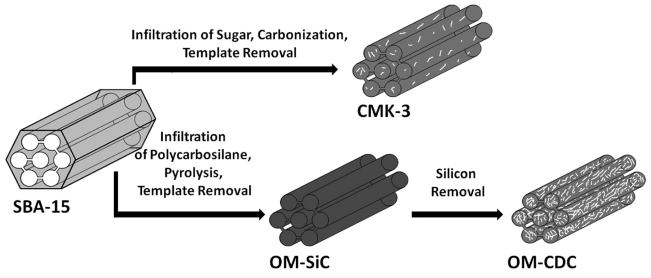

scattering as well as electron microscopy measurements.[22] The hierarchical pore structure of OM-CDC causes a very high apparent surface area ranging close to 2700 m^2/g and a total pore volume as high as 1.83 cm^3/g. The nitrogen physisorption isotherm of this sample exhibits a combination of type I and type IV contributions, according to the IUPAC classification (Figure 3). It shows a high N_2 uptake at low relative pressures

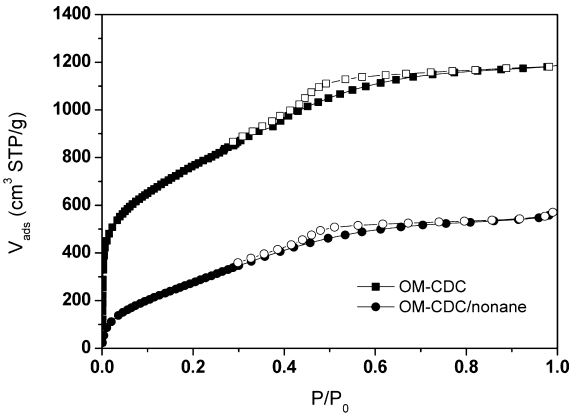

Figure 3. N_2 adsorption−desorption (filled symbols−empty symbols) isotherms at 77.4 K for ordered mesoporous carbide-derived carbon (OM-CDC) before and after *n*-nonane preadsorption.

($P/P_0 < 0.1$) and a distinct hysteresis loop located in the same relative pressure range as for the OM-SiC precursor material. In consequence, the effect of *n*-nonane preadsorption on this carbon material must be much more drastic compared to the almost exclusively (OM-SiC) and primarily (CMK-3) mesoporous materials. In fact, Figure 3 shows that 53% of the pore volume is blocked by *n*-nonane molecules resulting in a much lower uptake in the nitrogen physisorption after the hydrocarbon adsorption. However, because of the presence of large mesopore volumes, OM-CDC exhibits a high specific surface area of 1176 m^2/g even after *n*-nonane preadsorption, which is a value comparable to CMK-3 (859 m^2/g) and OM-SiC (723 m^2/g). In contrast to the mesoporous samples described above, the hydrocarbon saturation does not only decrease the nitrogen uptake of OM-CDC but also causes obvious changes in the hysteresis loop. On the one hand, saturation seems to occur at slightly lower relative pressures, and on the other hand, the total amount of condensed nitrogen is decreased. This phenomenon is attributed to the presence of *n*-nonane blocking the microporosity since part of the hydrocarbon chain points in the neighboring mesopores narrowing them in certain places. As described in the literature for ordered mesoporous silica

dx.doi.org/10.1021/la401206u | *Langmuir* 2013, 29, 8133−8139

materials, these newly developed constrictions modify the desorption mechanism, thus affecting the hysteresis loop.[23] In contrast to previously described lignocellulosic-derived activated carbons,[24] these results prove that there is a direct connection between the micro- and mesopores in OM-CDC, i.e., this material constitutes a real hierarchical structure, and accessibility limitations of the mesopores due to the blocked micropores can be ruled out.

In contrast to the hierarchical OM-CDC described above, a purely microporous CDC (micro-CDC) material shows a typical type I isotherm with high N_2 uptake at low relative pressure followed by the formation of a plateau due to complete saturation (see Figure 4). Because of the pure microporous nature of this sample, *n*-nonane blocks the pore volume almost completely (93%), and the amount of adsorbed nitrogen goes down close to zero, thus reflecting the absence of mesoporosity.

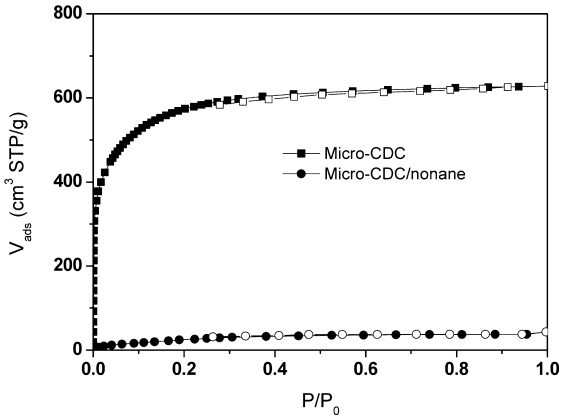

Figure 4. N_2 adsorption−desorption (filled symbols−empty symbols) isotherms at 77.4 K for microporous CDC before and after *n*-nonane preadsorption.

The effect of *n*-nonane preadsorption on the subsequent micropore filling mechanism can be more clearly discerned after comparing the different N_2 adsorption/desorption isotherms in logaritmic scale (see Figure S1, Supporting Information). On samples CMK-3, OM-CDC, and micro-CDC, the presence of *n*-nonane blocking the narrow micropores gives rise to a drastic decrease in the amount of nitrogen adsorbed at low relative pressures, i.e., the large adsorption potential on narrow micropores vanish due to the presence of *n*-nonane blocking these cavities.

In addition to nitrogen physisorption before and after *n*-nonane, CO_2 adsorption at 273 K and atmospheric pressure has been proposed for the characterization of the narrow microporous structure, i.e., these pores below 0.7−0.8 nm.[25] As it can be observed in the left panel of Figure 5, the amount of CO_2 adsorbed highly depends on the porous structure of the sample evaluated. Whereas CO_2 adsorption at atmospheric pressure ($P/P_0 \approx 0.03$) is very low for mainly mesoporous samples, i.e., SiC and CMK-3, it highly increases for samples containing a large proportion of narrow micropores. Interestingly, there is a good correlation between the volume of narrow micropores (pores below 0.7 nm), deduced after application of the Dubinin−Radushkevich (DR) equation to the CO_2 adsorption data, and the volume of pores blocked by *n*-nonane, estimated from the second nitrogen physisorption isotherm as described above (see right panel of Figure 5). The correlation between these two values confirms the preferential blocking of narrow micropores by *n*-nonane. However, the slight downward deviation for samples with a large narrow micropore volume (V_n) suggests the additional blocking of slightly larger micropores (<1.0 nm) by *n*-nonane. At this point, it is noteworthy to mention the absence of any correlation (not shown) with the total micropore volume (V_0) deduced from the N_2 adsorption data, thus confirming the ineffective blocking of large micropores (above ∼1.0 nm) using *n*-nonane.

To summarize the textural analysis using N_2 and CO_2 physisorption analysis, Table 1 reports the different textural parameters estimated before and after *n*-nonane preadsorption.

Previous studies reported in the literature have shown that Ar adsorption at 87.3 K is a very useful tool for a reliable and detailed characterization of the microporous structure on activated carbons.[26] The benefits of Ar versus N_2 adsorption can be summarized: (i) a higher relative pressure for micropore filling for Ar compared to N_2, due to weaker effective adsorption potential including the absence of specific interactions with the adsorbent surface, (ii) a higher boiling temperature (87.3 K) compared to nitrogen (77.4 K), which helps to reduce the presence of kinetic restrictions, in case narrow micropores are present, and (iii) a better description of the textural properties (pore size distribution and surface area

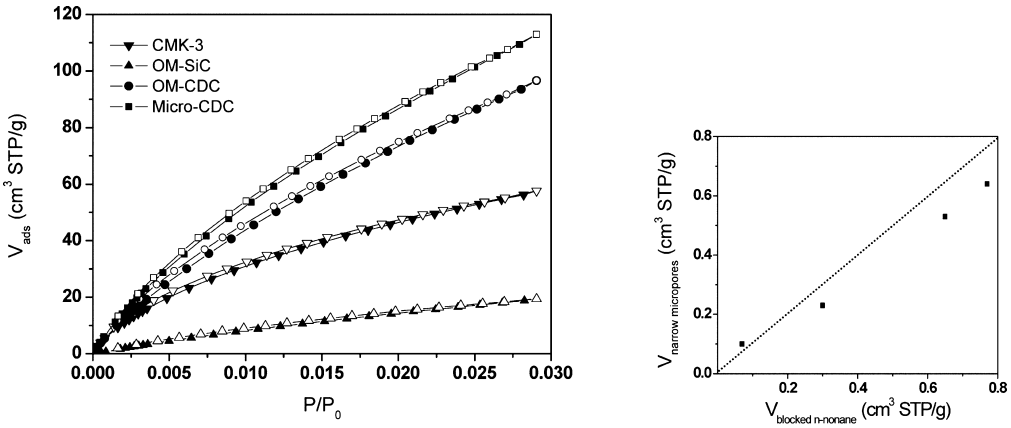

Figure 5. (Left) CO_2 adsorption−desorption (filled symbols−empty symbols) isotherms at 273 K for the different carbon materials (original SiC sample is also included). (Right) Correlation between the narrow micropore volume (V_n), calculated after application of the DR equation to the CO_2 adsorption data, and the volume of micropores blocked by *n*-nonane.

dx.doi.org/10.1021/la401206u | *Langmuir* 2013, 29, 8133−8139

analysis). The Ar physisorption isotherms for the different samples up to atmospheric pressure are in close agreement with N_2 adsorption measurements (Figure 6). Sample micro-CDC

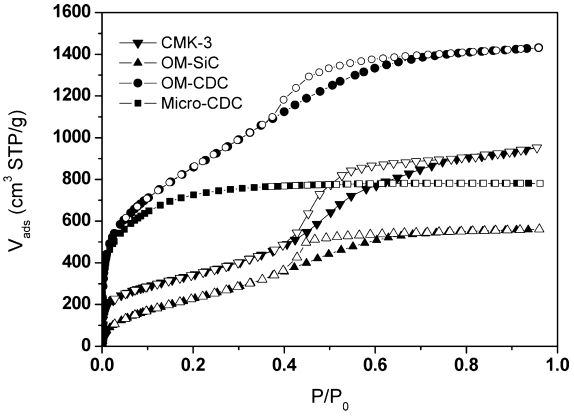

Figure 6. Ar adsorption−desorption (filled symbols−empty symbols) isotherms at 87.3 K for the different carbon materials and OM-SiC.

exhibits a type I isotherm as corresponds to a pure microporous material. OM-SiC and CMK-3 exhibit the capillary condensation in the mesopores at medium relative pressures ($P/P_0 \approx 0.4-0.6$), this phenomena being shifted to higher relative pressures on the CMK-3 sample due to the larger mesoporous size. Finally, sample OM-CDC combines a large micropore volume at low relative pressures due to the presence of micropores, together with a large capillary condensation on the mesopores at higher relative pressures.

As described above, Ar adsorption at 87.3 K is also a very useful tool for the characterization of the pore size distribution on carbon materials. The pore size distribution together with the cumulative pore volume for samples OM-SiC, CMK-3, OM-CDC, and micro-CDC (Figure 7) are deduced after application of the NLDFT method (cylindrical pore; equilibrium model) to the Ar adsorption data. As suggested from the slightly different positions of the hysteresis loops, the average mesopore size of CMK-3 (4.7 nm) is larger compared to OM-SiC (4.0 nm) as a result of the different precursor materials, either sugar or polycarbosilane polymer, which are infiltrated into the SBA-15 template. In close agreement with the nitrogen physisorption analyses before and after *n*-nonane preadsorption, the NLDFT pore size distributions show the presence of narrow micropores (0.7 nm) in the CMK-3, which is not the case for OM-SiC. A much more distinct microporosity is present in the OM-CDC. The PSD shows a certain amount of pores with a mean diameter of 0.9 nm located in the walls of the nanorods being typical for CDCs prepared from polycarbosilane precursors. The mesopore size of OM-CDC (3.3 nm) is comparable to the OM-SiC parent material as a result of the high conformability of the silicon

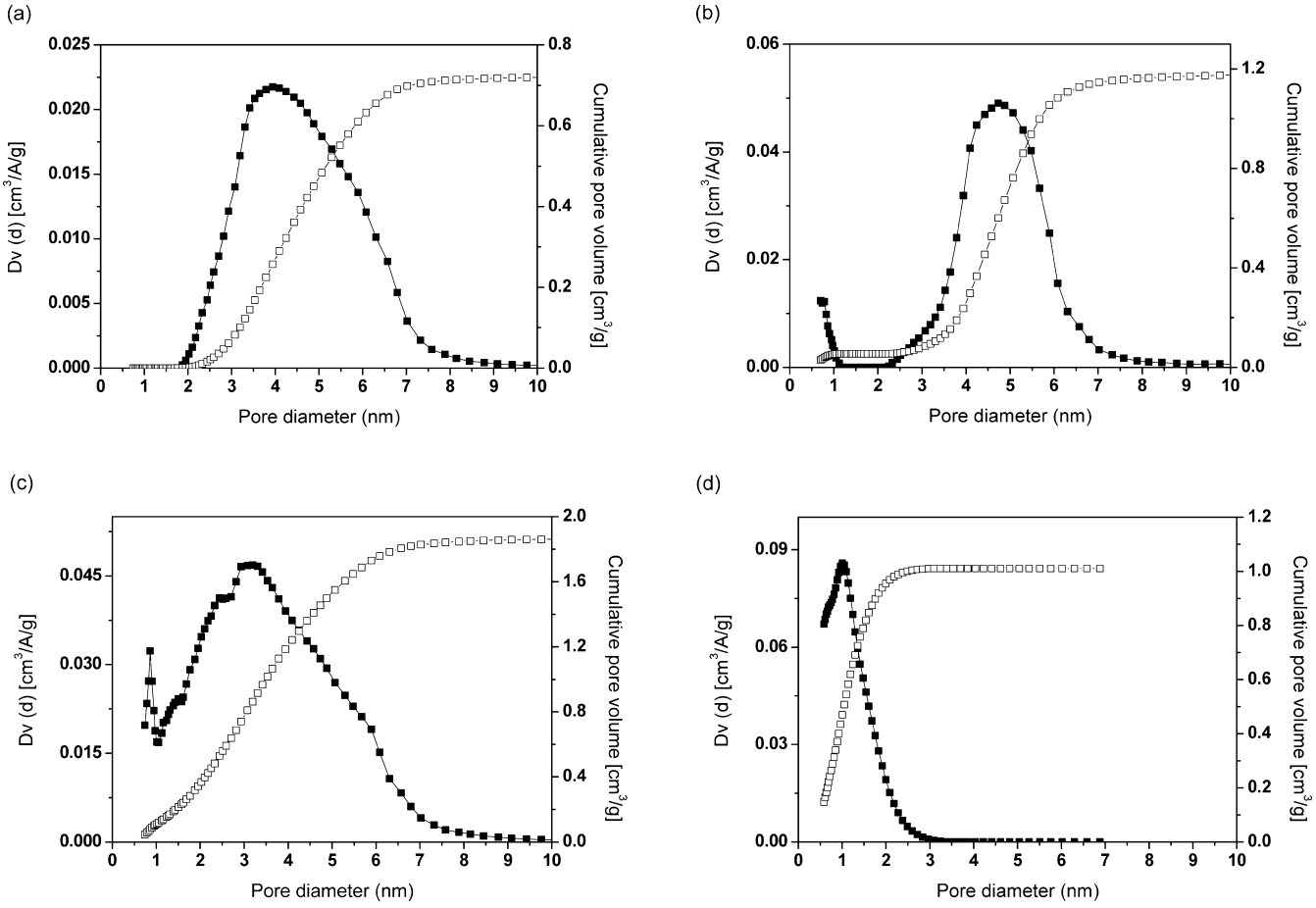

Figure 7. Pore size distribution (PSD) and cumulative pore volume for sample (a) OM-SiC, (b) CMK-3, (c) OM-CDC, and (d) micro-CDC after application of the NLDFT equilibrium model (cylindrical pore geometry) to the argon adsorption data at 87.3 K; for sample micro-CDC (slit-shape pore geometry), the QSDFT equilibrium model was used.

dx.doi.org/10.1021/la401206u | *Langmuir* 2013, 29, 8133−8139

extraction process. Nevertheless, a slight shrinkage can be observed since the average pore size shifts toward a lower value as compared to OM-SiC (4.0 nm). For sample micro-CDC, the pore size distribution was evaluated using the QSDFT method (slit-shape pore; equilibrium model) because no cylindrical mesopore system is present in this material. The average size of the micropores (1.0 nm) is in close agreement to OM-CDC because of the common procedure for the generation of these micropores under comparable conditions. The complete blocking of the microporosity on this sample by *n*-nonane (93% blocking) confirms that *n*-nonane preadsorption constitutes a useful tool for the characterization of the narrow microporous structure (pores below ∼1.0 nm) on carbon materials.

CONCLUSIONS

Physisorption of different gases and *n*-nonane preadsorption have been used for detailed analyses of the pore systems of ordered mesoporous materials CMK-3, OM-SiC, and OM-CDC as well as a microporous CDC reference material. Preadsorption of *n*-nonane combined with nitrogen physisorption at 77.4 K show that OM-SiC is almost exclusively mesoporous, whereas the carbon analogue CMK-3 contains a noticeable amount of micropores. Nitrogen uptakes before and after hydrocarbon saturation prove the presence of a real hierarchical pore structure in OM-CDC. The adsorption capacity of microporous CDC is reduced to zero after *n*-nonane preadsorption due to the complete blocking of the porosity and the absence of mesopores. The narrow micropores were also characterized with adsorption of carbon dioxide at 273 K and a good correlation was found between the pores below 0.7 nm, deduced after application of the Dubinin–Radushkevich (DR) equation to the CO_2 adsorption data, and the volume of pores blocked by *n*-nonane. The results of *n*-nonane preadsorption were corroborated by argon adsorption measurements at 87.3 K, which also proved to be a useful method for the characterization of the pore size distribution on the discussed materials.

ASSOCIATED CONTENT

Supporting Information

N_2 adsorption/desorption isotherms. This material is available free of charge via the Internet at http://pubs.acs.org.

AUTHOR INFORMATION

Corresponding Author

*E-mail: stefan.kaskel@chemie.tu-dresden.de (S.K.); joaquin.silvestre@ua.es (J.S.-A.).

Notes

The authors declare no competing financial interest.

REFERENCES

(1) Gogotsi, Y. *Carbon Nanomaterials*; CRC Press LLC: Boca Raton, FL, 2006.
(2) Xia, Y.; Yang, Z.; Mokaya, R. *Templated Porous Carbon Materials: Recent Developments*; John Wiley & Sons Ltd.: New York, 2011.
(3) Linares-Solano, A.; Cazorla-Amoros, D. *Adsorption on Activated Carbon Fibers*; Elsevier Ltd.: New York, 2008.
(4) Nishihara, H.; Kyotani, T. Templated nanocarbons for energy storage. *Adv. Mater.* **2012**, *24*, 4473–4498.
(5) Schüth, F.; Sing, K. S. W.; Weitkamp, J. *Handbook of Porous Solids*; Wiley-VCH Verlag GmbH & Co. KGaA: Berlin, Germany, 2002; Vol. 3.
(6) Taguchi, A.; Schüth, F. Ordered mesoporous materials in catalysis. *Microporous Mesoporous Mater.* **2004**, *77*, 1–45.
(7) Schloegl, R. *Handbook of Heterogeneous Catalysis*; Wiley-VCH: Weinheim, Germany, 2008.
(8) Simon, P.; Gogotsi, Y. Materials for electrochemical capacitors. *Nat. Mater.* **2008**, *7*, 845–854.
(9) Porada, S.; Weinstein, L.; Dash, R.; van der Wal, A.; Bryjak, M.; Gogotsi, Y.; Biesheuvel, P. M. Water desalination using capacitive deionization with microporous carbon electrodes. *ACS Appl. Mater. Interfaces* **2012**, *4*, 1194–1199.
(10) Hasegawa, G.; Kanamori, K.; Nakanishi, K.; Hanada, T. Fabrication of activated carbons with well-defined macropores derived from sulfonated poly(divinylbenzene) networks. *Carbon* **2010**, *48*, 1757–1766.
(11) Presser, V.; Heon, M.; Gogotsi, Y. Carbide-derived carbons: from porous networks to nanotubes and graphene. *Adv. Funct. Mater.* **2011**, *21*, 810–833.
(12) Gogotsi, Y.; Nikitin, A.; Ye, H.; Zhou, W.; Fischer, J. E.; Yi, B.; Foley, H. C.; Barsoum, M. W. Nanoporous carbide-derived carbon with tunable pore size. *Nat. Mater.* **2003**, *2*, 591–594.
(13) Osswald, S.; Portet, C.; Gogotsi, Y.; Laudisio, G.; Singer, J. P.; Fischer, J. E.; Sokolov, V. V.; Kukushkina, J. A.; Kravchik, A. E. Porosity control in nanoporous carbide-derived carbon by oxidation in air and carbon dioxide. *J. Solid State Chem.* **2009**, *182*, 1733–1741.
(14) Presser, V.; Yeon, S.-H.; Vakifahmetoglu, C.; Howell, C. A.; Sandeman, S. R.; Colombo, P.; Mikhalovsky, S.; Gogotsi, Y. Hierarchical porous carbide-derived carbons for the removal of cytokines from blood plasma. *Adv. Healthcare Mater.* **2012**, *1*, 796–800.
(15) Yushin, G.; Hoffman, E. N.; Barsoum, M. W.; Gogotsi, Y.; Howell, C. A.; Sandeman, S. R.; Phillips, G. J.; Lloyd, A. W.; Mikhalovsky, S. V. Mesoporous carbide-derived carbon with porosity tuned for efficient adsorption of cytokines. *Biomaterials* **2006**, *27*, 5755–5762.
(16) Lei, S.; Miyamoto, J.-I.; Kanoh, H.; Nakahigashi, Y.; Kaneko, K. Enhancement of the methylene blue adsorption rate for ultramicroporous carbon fiber by addition of mesopores. *Carbon* **2006**, *44*, 1884–1890.
(17) Tao, Y.; Kanoh, H.; Abrams, L.; Kaneko, K. Mesopore-modified zeolites: preparation, characterization, and applications. *Chem. Rev.* **2006**, *106*, 896–910.
(18) Jun, S.; Joo, S. H.; Ryoo, R.; Kruk, M.; Jaroniec, M.; Liu, Z.; Ohsuna, T.; Terasaki, O. Synthesis of New, Nanoporous Carbon with Hexagonally Ordered Mesostructure. *J. Am. Chem. Soc.* **2000**, *122*, 10712–10713.
(19) Kleitz, F.; Choi, S. H.; Ryoo, R. Cubic Ia3d large mesoporous silica: synthesis and replication to platinum nanowires, carbon nanorods and carbon nanotubes. *Chem. Commun.* **2003**, 2136–2137.
(20) Lu, A.-H.; Schüth, F. Nanocasting: a versatile strategy for creating nanostructured porous materials. *Adv. Mater.* **2006**, *18*, 1793–1805.
(21) Shi, Y.; Wan, Y.; Zhao, D. Ordered mesoporous non-oxide materials. *Chem. Soc. Rev.* **2011**, *40*, 3854–3878.
(22) Oschatz, M.; Kockrick, E.; Rose, M.; Borchardt, L.; Klein, N.; Senkovska, I.; Freudenberg, T.; Korenblit, Y.; Yushin, G.; Kaskel, S. A cubic ordered, mesoporous carbide-derived carbon for gas and energy storage applications. *Carbon* **2010**, *48*, 3987–3992.
(23) Silvestre-Albero, A.; Jardim, E. O.; Bruijn, E.; Meynen, V.; Cool, P.; Sepulveda-Escribano, A.; Silvestre-Albero, J.; Rodriguez-Reinoso, F. Is there any microporosity in ordered mesoporous silicas? *Langmuir* **2009**, *25*, 939–943.
(24) Silvestre-Albero, A.; Goncalves, M.; Itoh, T.; Kaneko, K.; Endo, M.; Thommes, M.; Rodriguez-Reinoso, F.; Silvestre-Albero, J. Well-defined mesoporosity on lignocellulosic-derived activated carbons. *Carbon* **2012**, *50*, 66–72.
(25) Garrido, J.; Linares-Solano, A.; Martin-Martinez, J. M.; Molina-Sabio, M.; Rodriguez-Reinoso, F.; Torregrosa, R. Use of nitrogen vs. carbon dioxide in the characterization of activated carbons. *Langmuir* **1987**, *3*, 76–81.

(26) Silvestre-Albero, J.; Silvestre-Albero, A.; Rodriguez-Reinoso, F.; Thommes, M. Physical characterization of activated carbons with narrow microporosity by nitrogen (77.4 K), carbon dioxide (273 K) and argon (87.3 K) adsorption in combination with immersion calorimetry. *Carbon* **2012**, *50*, 3128−3133.